Diffusion-Based Synthetic Brightfield Microscopy Images for Enhanced Single Cell Detection

Anonymous CVPR submission

Paper ID *****

Abstract

Accurate single cell detection in brightfield microscopy is crucial for biological research, yet data scarcity and annotation bottlenecks limit the progress of deep learning methods. We investigate the use of unconditional models to generate synthetic brightfield microscopy images and evaluate their impact on object detection performance. A U-Net based diffusion model was trained and used to create datasets with varying ratios of synthetic and real images. Experiments with YOLOv8, YOLOv9 and RT-DETR reveal that training with synthetic data achieves comparable, and in some cases, slightly improved detection accuracies at lower Intersection over Union (IoU) thresholds. A human expert survey demonstrates the high realism of generated images, with experts struggling to distinguish them from real microscopy images (accuracy ∼50%). Our findings suggest that diffusion-based synthetic data generation is a promising avenue for augmenting real datasets in microscopy image analysis, reducing the reliance on extensive manual annotation and potentially improving the robustness of cell detection models.

1. Introduction

Single cell detection in microscopy images is a fundamental task in biological and medical applications, enabling quantitative analysis of cellular processes and disease mechanisms [18]. Brightfield microscopy, a label-free technique, is widely used but presents challenges for automated analysis due to low contrast and variability in cell appearance [11]. Deep learning, particularly CNN-based object detectors, has shown great promise for automatic cell detection [3, 25]. However, the performance of these models is heavily dependent on large, annotated datasets, which are expensive and time-consuming to acquire in microscopy [21].

Synthetic data generation offers a potential solution to alleviate data scarcity. Recent advancements in diffusion models have demonstrated their ability to generate high-fidelity images across various domains [7, 22]. In microscopy, synthetic data could augment real datasets, improve model generalization, and reduce annotation efforts [12, 19, 26].

This paper explores the use of unconditional diffusion models for generating synthetic brightfield microscopy images and investigates their impact on single cell detection accuracy. We address the central research question: **Can synthetic brightfield microscopy images generated by diffusion models enhance the performance of object detection models for single cell detection?** We further investigate: (1) the perceptual realism of generated images through expert evaluation, and (2) the influence of synthetic data proportion in training datasets.

Our contributions include: (i) application of unconditional diffusion models for realistic brightfield microscopy image synthesis; (ii) a comprehensive evaluation of synthetic data augmentation for single cell detection using state-of-the-art object detectors (YOLOv9, YOLOv9, RT-DETR); (iii) expert validation of generated image realism; and (iv) insights into the potential and limitations of diffusion-based synthetic data for microscopy image analysis.

2. Related Work

Synthetic microscopy image generation has gained traction for data augmentation and algorithm development. Early methods employed rule-based models and physical simulations [19, 23, 24], often limited by their ability to capture complex biological diversity.

Deep learning-based generative models, particularly GANs and diffusion models, have emerged as powerful alternatives. GANs have been used for cross-modality translation [1, 5, 6], super-resolution [28], and cell image generation [17]. However, GAN training can be unstable and prone to mode collapse [10, 20].

Diffusion models, inspired by non-equilibrium thermodynamics [8], offer improved training stability and sample

quality [7, 22]. Applications in microscopy include painting image generation [2], super-resolution [4], electron microscopy enhancement [15], and physics-informed reconstruction [13].

While diffusion models are increasingly used in microscopy image generation, research on their direct application for enhancing **object detection** in brightfield microscopy remains limited. This work addresses this gap by systematically evaluating the impact of diffusion-based synthetic brightfield microscopy image data on single cell detection performance using state-of-the-art object detection models.

3. Methodology

Our methodology comprises two main stages: (1) unconditional diffusion model training and synthetic image generation, and (2) evaluation of object detection models trained with varying proportions of synthetic data.

3.1. Image Generation with Diffusion Models

We trained an unconditional diffusion model with a U-Net architecture [21] using a dataset of 10,000 patches (512×512) extracted from real brightfield microscopy images of stably transfected CHO cells (see supplementary material for dataset details). The U-Net architecture consisted of down and up-sampling blocks with residual connections and optionally attention mechanisms in the down and up-sampling paths. We employed the DDIM scheduler [22] for efficient sampling and trained the model for 350 epochs using the AdamW optimizer with a learning rate of $1e^{-4}$. Model selection was based on visual inspection of generated samples and the Fréchet Inception Distance (FID) scores calculated against a held-out set of real images. The final generation process used the Euler a scheduler with trailing timestep spacing and epsilon prediction type, generating images with inference steps randomized between 35 and 40.

3.2. Cell Detection Model Training and Evaluation

We created six datasets containing synthetic images and a baseline dataset containing 5,000 real images (*scc_real*), that is used to compare the performance of the detection models trained with synthetic data. Three datasets used varying proportions of synthetic images (10%, 30%, and 50%) to replace real images in the training set (*scc_10*, *scc_30*, *scc_50*), while the remaining three datasets used the same proportions to add synthetic images to the training set (*scc_add_10*, *scc_add_30*, *scc_add_50*). Real images were labeled using a semi-automated approach combining fluorescence channel information and manual verification. Synthetic images were labeled using model-assisted labeling with a pre-trained and fine-tuned YOLOv8m model and manual label refinement.

We fine-tuned three state-of-the-art object detection models: YOLOv8 (sizes s, m, x) [9], YOLOv9 (sizes c, e) [27], and RT-DETR (sizes l, x) [16], pre-trained on COCO [14]. Models were trained for 200 epochs using default Ultralytics augmentation settings and evaluated on a held-out test set of 16,758 real images. Performance was measured using mean Average Precision (mAP) at IoU thresholds of 0.5 (mAP50), 0.75 (mAP75), and averaged across IoUs from 0.5 to 0.95 (mAP50:95).

3.3. Expert Survey for Image Realism

To assess the perceptual realism of generated images, we conducted a survey with 11 microscopy experts and biologists from Synentec GmbH. Participants were presented with 30 randomly ordered images (20 synthetic, 10 real) and asked to classify each as real or generated and rate their confidence. We analyzed classification accuracy and collected textual explanations for misclassifications to understand the visual cues experts relied upon.

4. Experiments and Results

4.1. Expert Survey: Indistinguishability of Synthetic Images

The expert survey results revealed a striking inability of microscopy experts to consistently distinguish synthetic brightfield microscopy images generated by our diffusion model from real images. The overall classification accuracy all 11 participants and 30 images was remarkably close to chance level, reaching only 50%. This near-random performance strongly indicates the high degree of realism achieved by our synthetic image generation approach. Figure 1 presents the normalized confusion matrix, visually demonstrating the balanced distribution of correct and incorrect classifications for both real and generated images. Individual image accuracies varied significantly, ranging from approximately 18% to 90%, highlighting the inherent variability within both real and synthetic image sets and the complexity of the discrimination task. Analysis of expert explanations revealed that experts considered subtle image features related to cell appearance, background texture, edge clarity, and perceived noise or artifacts when attempting to differentiate the images. Prominent terms like "cell," "background," and "edge" indicate a focus on core microscopy image components, while terms such as "pattern," "perfect," "artifacts," "blurry," and "contrast" suggested that experts were searching for subtle imperfections or stylistic inconsistencies that might betray a synthetic origin. However, these cues proved unreliable, ultimately leading to the near-chance level classification accuracy and underscoring the perceptual realism of our diffusion-generated brightfield microscopy images.

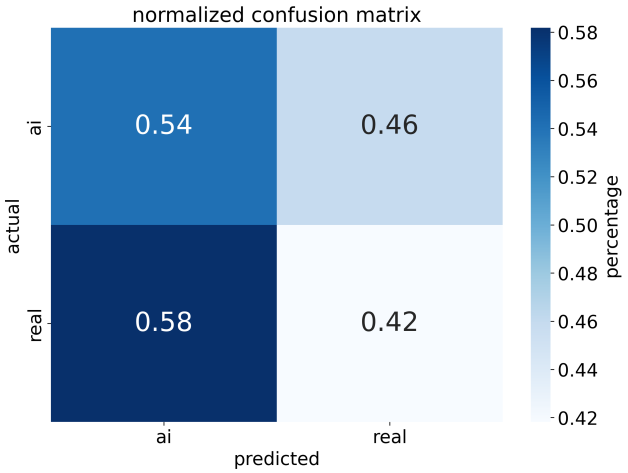

Figure 1. Normalized confusion matrix of expert survey classifications. Overall accuracy is approximately 50%, demonstrating the significant difficulty for experts in distinguishing real and synthetic brightfield microscopy images.

4.2. Object Detection Performance

Table 1 summarizes the object detection performance, presenting mAP metrics for all trained models across the seven datasets. Analyzing mAP50, we observe that models trained with synthetic data replacing parts of the real data (*scc_10*, *scc_30*, *scc_50*) achieve comparable, and in some cases, slightly improved performance compared to models trained solely on real data (*scc_real*). Specifically, the YOLOv8s model trained on the *scc_30* dataset achieved a mAP50 of 0.9043, marginally exceeding the 0.8947 achieved by the same model trained on the *scc_real* dataset. Similarly, the RT-DETR-l model trained on the *scc_10* dataset reached a mAP50 of 0.9147, very slightly outperforming the 0.9146 achieved on the *scc_real* dataset. These results suggest that synthetic data augmentation can maintain or even slightly enhance detection performance at lower IoU thresholds, potentially due to increased data variability and improved model robustness.

However, when examining performance at higher IoU thresholds, specifically mAP75 and mAP50:95, a subtle trend of performance decrease merges for models trained with increasing proportions of synthetic data. This trend is more pronounced for the RT-DETR models, indicating a potentially greater sensitivity of transformer-based architectures to the characteristics of synthetic data.

Qualitative assessment of sample detections (examples in supplementary material) revealed that all models, including those trained with synthetic data, generally performed well in detecting cells under diverse conditions, including overlapping cells and cells at image boundaries. However, subtle differences in detection precision and confidence scores were observed, warranting further investigation into the fine-grained impact of synthetic data on model behavior.

Table 1. Detailed comparison of the performance metrics for all evaluated models across the different training datasets.

Model	Dataset	mAP @50	mAP @75	mAP @50:95
YOLOv8s	*scc_real*	0.8947	0.8095	0.6557
	scc_10	0.8941	0.8053	0.6470
	scc_30	0.9043	0.8079	0.6448
	scc_50	0.8932	0.7891	0.6325
	scc_add_10	0.8949	0.8068	0.6502
	scc_add_30	0.8952	0.8115	0.6536
	scc_add_50	0.8940	0.8100	0.6514
YOLOv8m	*scc_real*	0.9038	0.8203	0.6637
	scc_10	0.9035	0.8093	0.6558
	scc_30	0.8945	0.8076	0.6462
	scc_50	0.8930	0.8040	0.6456
	scc_add_10	0.8943	0.8088	0.6550
	scc_add_30	0.9034	0.8224	0.6606
	scc_add_50	0.8950	0.8218	0.6588
YOLOv8x	*scc_real*	0.9038	0.8120	0.6639
	scc_10	0.9032	0.8055	0.6531
	scc_30	0.9031	0.8085	0.6549
	scc_50	0.8935	0.7961	0.6425
	scc_add_10	0.8941	0.8090	0.6560
	scc_add_30	0.8942	0.8212	0.6639
	scc_add_50	0.8938	0.8195	0.6440
YOLOv9c	*scc_real*	0.9047	0.8215	0.6645
	scc_10	0.9042	0.8070	0.6531
	scc_30	0.9042	0.8106	0.6568
	scc_50	0.8935	0.7951	0.6422
	scc_add_10	0.8954	0.8211	0.6615
	scc_add_30	0.8952	0.8217	0.6605
	scc_add_50	0.8947	0.8102	0.6594
YOLOv9e	*scc_real*	0.9037	0.8201	0.6629
	scc_10	0.9041	0.8141	0.6650
	scc_30	0.8946	0.8069	0.6485
	scc_50	0.8938	0.8037	0.6453
	scc_add_10	0.8950	0.8188	0.6623
	scc_add_30	0.8952	0.8209	0.6638
	scc_add_50	0.9031	0.8188	0.6651
RT-DETR-l	*scc_real*	0.9146	0.8169	0.6614
	scc_10	0.9147	0.8071	0.6574
	scc_30	0.9017	0.7780	0.6240
	scc_50	0.9036	0.7843	0.6298
	scc_add_10	0.9146	0.8064	0.6526
	scc_add_30	0.9043	0.7962	0.6457
	scc_add_50	0.9036	0.7932	0.6372
RT-DETR-x	*scc_real*	0.9164	0.8257	0.6748
	scc_10	0.9144	0.8083	0.6565
	scc_30	0.9032	0.7830	0.6328
	scc_50	0.9045	0.8032	0.6437
	scc_add_10	0.9133	0.7991	0.6459
	scc_add_30	0.9136	0.8106	0.6532
	scc_add_50	0.9012	0.7682	0.6203

5. Discussion

The expert survey results provide compelling evidence for the high perceptual realism of brightfield microscopy images generated by our unconditional diffusion model. The near-chance level accuracy achieved by microscopy experts in distinguishing synthetic images from real ones strongly support the notion that diffusion models can effectively synthesize microscopy data that is visually indistinguishable from real-world acquisitions. This finding directly addresses our first sub-research question and highlights the potential of diffusion models to generate data suitable for augmenting or even substituting real microscopy images in certain applications.

Object detection experiments further reveal the practical utility of diffusion-based synthetic data for single cell detection. The comparable, and in some cases, slightly improved performance of models trained with synthetic data augmentation at mAP50 demonstrates that synthetic images can effectively capture essential cell features and spatial distributions relevant for accurate cell localization. This directly addresses our main research question and suggests that synthetic data can be a valuable asset in training robust cell detection models, particularly when labeled real data is limited. The slight performance enhancement observed at mAP50 for some models might be attributed to the increased variability introduced by the synthetic data generation process, potentially improving model generalization and robustness to variations in real-world microscopy images.

However, the subtle performance decrease observed at higher IoU thresholds (mAP75, mAP50:95) for models trained with higher proportions of synthetic data indicates a potential limitation in the fidelity of synthetic images for fine cell boundary details and precise localization. This suggests that while diffusion models excel at generating perceptually realistic images capturing overall cell appearance and context, replicating the subtle nuances of cell morphology and edge definition present in real microscopy images remains a challenge for future refinement. The observed sensitivity of RT-DETR models to synthetic data proportion also warrants further investigation, potentially indicating architectural differences in how transformer-based models learn from and generalize with synthetic data compared to CNN-based YOLO models.

The implications of our findings for biological research and applications are two-fold. The demonstrated ability to generate high-quality synthetic brightfield microscopy images and effectively utilize them for training cell detection models opens up new avenues for addressing data scarcity and annotation bottlenecks in microscopy image analysis. Synthetic data generation offers a cost-effective and scalable approach to augment limited real datasets, potentially democratizing access to advanced cell detection techniques, particularly for research groups with limited biological resources or access to large annotated datasets. Furthermore, the use of synthetic data can reduce the dependence on time-consuming and expensive manual labor work, saving time and resources researcher usually have to invest in the laboratorial process. The potential to reduce or eliminate the need for fluorescent labels in certain applications, by relying on robust detection models trained with label-free brightfield images augmented by synthetic data, also aligns with ethical considerations and best practices in cell biology, minimizing potential cytotoxic effects and enabling more physiologically relevant live-cell imaging studies. Moreover, synthetic data generation offers the unique capability to create diverse datasets encompassing rare cell phenotypes or challenging imaging conditions that are difficult to obtain in real-world experiments, potentially enhancing the robustness nad generalizability of cell detection models for a wider range of biological applications and scenarios. Transparency in reporting the use of synthetic data in research is crucial for maintaining scientific rigor and ethical standards, ensuring appropriate interpretation and validation of findings derived from models trained with synthetic data augmentation.

6. Conclusion

This paper provides a comprehensive investigation into the use of diffusion-based synthetic brightfield microscopy images for enhancing single cell detection. Our expert survey demonstrates the remarkable realism of diffusion-generated images, achieving near-indistinguishability from real microscopy acquisitions. Object detection experiments reveal that models trained with synthetic data achieve comparable, and in some cases, slightly improved performance to real-data training, particularly for simpler cell localization (mAP50). While subtle limitations exist in replicating fine cell boundary details and achieving optimal performance at higher IoU thresholds, our findings strongly highlight the promise of diffusion-based synthetic data generation as a valuable tool for microscopy image analysis. This approach offers a pathway to address data scarcity, reduce annotation burdens, and potentially improve the robustness and accessibility of advanced cell detection techniques in biological and medical research. Future research directions should focus on refining diffusion models for brightfield microscopy image generation, improving the fidelity in capturing fine cellular details, exploring conditional generation strategies for broader applicability across diverse microscopy modalities and biological contexts, and further investigating the optimal strategies for integrating synthetic data into training pipelines to maximize the benefits for cell detection and other microscopy image analysis tasks.

References

[1] Eric M. Christiansen, Samuel J. Yang, D. Michael Ando, Ashkan Javaherian, Gaia Skibinski, Scott Lipnick, Elliot Mount, Alison O'Neil, Kevan Shah, Alicia K. Lee, Piyush Goyal, William Fedus, Ryan Poplin, Andre Esteva, Marc Berndl, Lee L. Rubin, Philip Nelson, and Steven Finkbeiner. In Silico Labeling: Predicting Fluorescent Labels in Unlabeled Images. *Cell*, 173(3):792–803.e19, 2018. 1

[2] Jan Oscar Cross-Zamirski, Praveen Anand, Guy Williams, Elizabeth Mouchet, Yinhai Wang, and Carola-Bibiane Schönlieb. Class-Guided Image-to-Image Diffusion: Cell Painting from Brightfield Images with Class Labels, 2023. arXiv:2303.08863 [cs, q-bio]. 2

[3] Erick Moen, Erick K. Moen, Erick Moen, Dylan Bannon, Dylan Bannon, Tetsuichi Kudo, Takamasa Kudo, William D. Graf, William Graf, Markus W. Covert, Markus W. Covert, David Van Valen, and David Van Valen. Deep learning for cellular image analysis. *Nature Methods*, 16(12):1233–1246, 2019. MAG ID: 2946901414. 1

[4] Gabriel della Maggiora, L. A. Croquevielle, Nikita Desphande, Harry Horsley, Thomas Heinis, and Artur Yakimovich. Conditional Variational Diffusion Models. *arXiv.org*, 2023. ARXIV_ID: 2312.02246 S2ID: 0aa948324bca48784d2a78a799c92b101687c89e. 2

[5] Gyuhyun Lee, Gyuhyun Lee, Jeong-Woo Oh, Jeong-Woo Oh, Mi-Sun Kang, Mi-Sun Kang, Nam-Gu Her, Nam-Gu Her, Myoung-Hee Kim, Myoung-Hee Kim, Won-Ki Jeong, and Won-Ki Jeong. DeepHCS: Bright-Field to Fluorescence Microscopy Image Conversion Using Deep Learning for Label-Free High-Content Screening. *International Conference on Medical Image Computing and Computer-Assisted Intervention*, pages 335–343, 2018. MAG ID: 2892296896 S2ID: 6221dc0f12e1513610a3a4de8b1fc4adff628825. 1

[6] Gyuhyun Lee, Gyuhyun Lee, Jeong-Woo Oh, Jeong-Woo Oh, Jeong-Woo Oh, Nam-Gu Her, Nam-Gu Her, Won-Ki Jeong, and Won-Ki Jeong. DeepHCS++: Bright-field to fluorescence microscopy image conversion using multi-task learning with adversarial losses for label-free high-content screening. *Medical Image Analysis*, 70:101995, 2021. MAG ID: 3133306532 S2ID: 6ba26fb5c73049bf60d365a19be4cc209c4f917e. 1

[7] Jonathan Ho, Ajay Jain, and Pieter Abbeel. Denoising Diffusion Probabilistic Models, 2020. arXiv:2006.11239 [cs, stat]. 1, 2

[8] Jascha Sohl-Dickstein, Jascha Sohl-Dickstein, Eric A. Weiss, Eric L. Weiss, Niru Maheswaranathan, Niru Maheswaranathan, Surya Ganguli, and Surya Ganguli. Deep Unsupervised Learning using Nonequilibrium Thermodynamics. *arXiv: Learning*, 2015. ARXIV_ID: 1503.03585 MAG ID: 2129069237 S2ID: 2dcef55a07f8607a819c21fe84131ea269cc2e3c. 1

[9] Glenn Jocher, Ayush Chaurasia, and Jing Qiu. Ultralytics YOLO, 2023. original-date: 2022-09-11T16:39:45Z. 2

[10] Juan C Caicedo, Juan C. Caicedo, Jonathan Roth, Jonathan R. Roth, Allen Goodman, Allen Goodman, Tim Becker, Tim Becker, Tim Becker, Kyle W. Karhohs, Kyle W. Karhohs, Matthieu Broisin, Matthieu Broisin, Csaba Molnár, Csaba Molnar, Claire McQuin, Claire McQuin, Shantanu Singh, Shantanu Singh, Fabian J. Theis, Fabian J. Theis, Anne E. Carpenter, and Anne E. Carpenter. Evaluation of Deep Learning Strategies for Nucleus Segmentation in Fluorescence Images. *Cytometry Part A*, 95(9):952–965, 2019. MAG ID: 2961912654. 1

[11] Jyrki Selinummi, Jyrki Selinummi, Pekka Ruusuvuori, Pekka Ruusuvuori, Irina Podolsky, Irina Podolsky, Irina Podolsky, Adrian Ozinsky, Adrian Ozinsky, Elizabeth S. Gold, Elizabeth S. Gold, Olli Yli-Harja, Olli Yli-Harja, Alan Aderem, Alan Aderem, Ilya Shmulevich, and Ilya Shmulevich. Bright Field Microscopy as an Alternative to Whole Cell Fluorescence in Automated Analysis of Macrophage Images. *PLOS ONE*, 4(10), 2009. MAG ID: 1980189947 S2ID: 26af3e90694e8ed14e25a11f0492af6b2e39ca87. 1

[12] A. Lehmussola, P. Ruusuvuori, J. Selinummi, T. Rajala, and O. Yli-Harja. Synthetic Images of High-Throughput Microscopy for Validation of Image Analysis Methods. *Proceedings of the IEEE*, 96(8):1348–1360, 2008. 1

[13] Rui Li, Gabriel della Maggiora, Vardan Andriasyan, Anthony Petkidis, Artsemi Yushkevich, Mikhail Kudryashev, and Artur Yakimovich. Microscopy image reconstruction with physics-informed denoising diffusion probabilistic model, 2023. Version Number: 2. 2

[14] Tsung-Yi Lin, Michael Maire, Serge J. Belongie, Lubomir D. Bourdev, Ross B. Girshick, James Hays, Pietro Perona, Deva Ramanan, Piotr Dollár, and C. Lawrence Zitnick. Microsoft COCO: common objects in context. *CoRR*, abs/1405.0312, 2014. 2

[15] Chixiang Lu, Kai Chen, Heng Qiu, Xiaojun Chen, Gu Chen, Xiaojuan Qi, and Haibo Jiang. Diffusion-based deep learning method for augmenting ultrastructural imaging and volume electron microscopy. *Nature Communications*, 15(1): 4677, 2024. 2

[16] Wenyu Lv, Shangliang Xu, Yian Zhao, Guanzhong Wang, Jinman Wei, Cheng Cui, Yuning Du, Qingqing Dang, and Yi Liu. DETRs beat yolos on real-time object detection. *ArXiv*, abs/2304.08069, 2023. 2

[17] Marin Scalbert, Marin Scalbert, Florent Couzinié-Devy, Florent Couzinie-Devy, Riadh Fezzani, and Riadh Fezzani. Generic Isolated Cell Image Generator. *Cytometry Part A*, 95(11), 2019. MAG ID: 2979953123. 1

[18] Erik Meijering. Cell Segmentation: 50 Years Down the Road [Life Sciences]. *IEEE Signal Processing Magazine*, 29(5): 140–145, 2012. 1

[19] Satwik Rajaram, Benjamin Pavie, Nicholas E F Hac, Steven J Altschuler, and Lani F Wu. SimuCell: a flexible framework for creating synthetic microscopy images. *Nature Methods*, 9(7):634–635, 2012. 1

[20] Ricard Durall, Ricard Durall, Avraam Chatzimichailidis, Avraam Chatzimichailidis, Peter Labus, Peter Labus, Peter Labus, Peter Labus, Janis Keuper, and Janis Keuper. Combating Mode Collapse in GAN training: An Empirical Analysis using Hessian Eigenvalues. *arXiv: Learning*, 2020. ARXIV_ID: 2012.09673 MAG ID: 3112865286 S2ID: 3ad13bd6713d74eec7faa964050f7d61089440a0. 1

[21] Olaf Ronneberger, Philipp Fischer, and Thomas Brox. U-Net: Convolutional Networks for Biomedical Image

Segmentation. *arXiv:1505.04597 [cs]*, 2015. arXiv: 1505.04597. 1, 2

[22] Jiaming Song, Chenlin Meng, and Stefano Ermon. Denoising Diffusion Implicit Models. *CoRR*, 2020. Publisher: arXiv Version Number: 4. 1, 2

[23] David Svoboda and Vladimír Ulman. Generation of synthetic image datasets for time-lapse fluorescence microscopy. In *Image Analysis and Recognition*, pages 473–482, Berlin, Heidelberg, 2012. Springer Berlin Heidelberg. 1

[24] David Svoboda and Vladimír Ulman. Towards a realistic distribution of cells in synthetically generated 3d cell populations. In *Image Analysis and Processing – ICIAP 2013*, pages 429–438, Berlin, Heidelberg, 2013. Springer Berlin Heidelberg. 1

[25] Thorsten Falk, Thorsten Falk, Dominic Mai, Dominic Mai, Robert Bensch, Robert Bensch, Özgün Çiçek, Özgün Çiçek, Ahmed Abdulkadir, Ahmed Abdulkadir, Yassine Marrakchi, Yassine Marrakchi, Anton Böhm, Anton Böhm, Jan Deubner, Jan Deubner, Zoë Jäckel, Zoe Jäckel, Katharina Seiwald, Katharina Seiwald, Alexander Dovzhenko, Alexander Dovzhenko, Olaf Tietz, Olaf Tietz, Cristina Dal Bosco, Cristina Dal Bosco, Seán Walsh, Sean Walsh, Deniz Saltukoglu, Deniz Saltukoglu, Tuan Leng Tay, Tuan Leng Tay, Marco Prinz, Marco Prinz, Klaus Palme, Klaus Palme, Klaus Palme, Matias Simons, Matias Simons, Ilka Diester, Ilka Diester, Thomas Brox, Thomas Brox, Olaf Ronneberger, and Olaf Ronneberger. U-Net: deep learning for cell counting, detection, and morphometry. *Nature Methods*, 16(1): 67–70, 2019. MAG ID: 2900936384. 1

[26] Patrick Trampert, Dmitri Rubinstein, Faysal Boughorbel, Christian Schlinkmann, Maria Luschkova, Philipp Slusallek, Tim Dahmen, and Stefan Sandfeld. Deep Neural Networks for Analysis of Microscopy Images—Synthetic Data Generation and Adaptive Sampling. *Crystals*, 11(3):258, 2021. 1

[27] Chien-Yao Wang, I-Hau Yeh, and Hongpeng Liao. YOLOv9: Learning what you want to learn using programmable gradient information. *ArXiv*, abs/2402.13616, 2024. 2

[28] Hao Zhang, Chunyu Fang, Xinlin Xie, Yicong Yang, Wei Mei, Di Jin, and Peng Fei. High-throughput, high-resolution deep learning microscopy based on registration-free generative adversarial network. *Biomedical Optics Express*, 10(3): 1044, 2019. 1